



ИНЖЕНЕРИЯ ЖӘНЕ ИНЖЕНЕРЛІК ІС  
ИНЖЕНЕРИЯ И ИНЖЕНЕРНОЕ ДЕЛО  
ENGINEERING AND ENGINEERING

ИНЖЕНЕРИЯ ЖӘНЕ ИНЖЕНЕРЛІК ІС  
ИНЖЕНЕРИЯ И ИНЖЕНЕРНОЕ ДЕЛО  
ENGINEERING AND ENGINEERING

DOI 10.51885/1561-4212\_2025\_2\_20  
IRSTI 29.19.23

A.S. Zhakypov<sup>1,2</sup>, T.N. Zhumanov<sup>2</sup>, N.Y. Akhanova<sup>1</sup>, M.N. Sultangazina<sup>2</sup>, M.T. Gabdullin<sup>1</sup>

<sup>1</sup>Kazakh-British Technical University, Almaty, Kazakhstan

<sup>2</sup>al-Farabi Kazakh National University, Almaty, Kazakhstan

E-mail: [szhakupovalibek@gmail.com](mailto:szhakupovalibek@gmail.com)

E-mail: [szhakupovalibek@gmail.com](mailto:szhakupovalibek@gmail.com)

E-mail: [nazym@physics.kz](mailto:nazym@physics.kz)

E-mail: [marjan\\_0309@mail.ru](mailto:marjan_0309@mail.ru)\*

E-mail: [m.gabdullin@kbtu.kz](mailto:m.gabdullin@kbtu.kz)

### ГЕЛЬМГОЛЬЦ КАТУШКА ГЕОМЕТРИЯСЫНЫҢ МАГНИТ ӨРІСІНІҢ ШАМАСЫ МЕН БІРТЕКТІЛІГІНЕ ӘСЕРІ

### THE INFLUENCE OF HELMHOLTZ COIL GEOMETRY ON THE MAGNITUDE AND HOMOGENEITY OF THE MAGNETIC FIELD

### ВЛИЯНИЕ ГЕОМЕТРИИ КАТУШКИ ГЕЛЬМГОЛЬЦА НА ВЕЛИЧИНУ И ОДНОРОДНОСТЬ МАГНИТНОГО ПОЛЯ

**Abstract.** Creating installations capable of generating a stable and controllable homogeneous magnetic field is a complex and urgent technical task in the field of applied engineering. Controlling the magnetic field enables efficient manipulation of ferromagnetic micro- and nanoparticles, which opens up applications of homogeneous magnetic fields in magnetic separation, sensor calibration, and artificial compensation of the Earth's magnetic field. One of the new areas of application of such a homogeneous magnetic field is the magnetic separation of ferromagnetic micro- and nanoparticles. A Helmholtz coil is the most popular technology for creating and controlling a stable homogeneous magnetic field, consisting of two coaxial identical coils separated by a distance equal to their radius. Today, this technology is used in many areas of scientific research and technical applications. Geometrical configurations of the Helmholtz coil such as the shape, number of turns, and spacing between them, have a significant effect on both the magnitude of the magnetic field and its homogeneity. In this paper, theoretical calculations are performed comparing the effect of the geometry of round and square Helmholtz coils on the homogeneity and magnitude of the magnetic field. The calculations took into account the thickness of the coils and the arrangement of the turns. The results showed that the value of the homogeneity zone of the round coil is larger than that of the square coil, but the magnetic induction in this zone is larger for the square coil than for the round coil. When taking into account the thickness, the difference between the coils is smaller than without taking into account the thickness. In further studies, the obtained theoretical calculations of the distribution of the magnetic induction of the Helmholtz coil will be used to analyze the experimental data. Also, based on these calculations, a laboratory prototype for magnetic separation based on the Helmholtz coil will be developed.

**Keywords:** Helmholtz coil, Biot-Savart-Laplace law, magnetic field homogeneity, magnetic field generator, computational model, coil geometry

**Аңдатпа.** Тұрақты және басқарылатын біртекті магнит өрісін құруға қабілетті қондырғыларды құру күрделі және шұғыл техникалық міндет болып табылады. Осындай біртекті магнит өрісін қолданудың жаңа бағыттарының бірі микро- және наноөлшемді ферромагниттік

бөлшектердің магниттік бөлінуі болып табылады. Гельмгольц катушкасы тұрақты біртекті магнит өрісін құруға және басқаруға арналған ең танымал технология болып табылады. Бұл технология ғылыми зерттеулер мен техникалық қолданудың көптеген салаларында қолданылады. Гельмгольц катушкасының геометриялық конфигурациялары магнит өрісінің шамасына да, оның біртектілігіне де әсер етеді. Бұл жұмыста дөңгелек және шаршы Гельмгольц катушкаларының геометриясының магнит өрісінің біртектілігі мен шамасына әсерін салыстыратын теориялық есептеулер орындалады. Есептеулер катушкалардың қалыңдығын және бұрылыстардың орналасуын ескерді. Нәтижелер шаршы катушканың магнит өрісінің абсолютті мәні дөңгелек катушкаға қарағанда жоғары екенін көрсетті. Дегенмен, дөңгелек Гельмгольц катушкасы магнит өрісінің жақсы біртектілігін көрсетті.

**Түйін сөздер:** Гельмгольц орамы, Био-Саварт-Лаплас заңы, магнит өрісінің біртектілігі, магнит өрісінің генераторы, есептеу моделі

**Аннотация.** Создание установок, способных генерировать стабильное и управляемое однородное магнитное поле, является сложной и актуальной технической задачей в области прикладной инженерии. Управление магнитным полем дает возможность эффективно контролировать ферромагнитные микро- и наночастицы, что дает возможность применения однородного магнитного поля в области магнитной сепарации, калибровки сенсоров и искусственного обнуления магнитного поля Земли. Катушка Гельмгольца является самой популярной технологией создания и управления стабильным однородным магнитным полем, состоящая из двух соосных катушек, расстояние между которыми равно их радиусу. На сегодняшний день данная технология используется во многих областях научных исследований и технических приложений. Геометрические конфигурации катушки Гельмгольца, такие как форма, количество витков и расстояние между ними, оказывают существенное влияние как на величину магнитного поля, так и на его однородность. В данной работе выполнены теоретические расчеты, сравнивающие влияние геометрии круглых и квадратных катушек Гельмгольца на однородность и величину магнитного поля. При расчетах учитывалась толщина катушек и расположение витков. Результаты показали, что величина зоны однородности круглой катушки больше, чем у квадратной, но магнитная индукция в этой зоне больше у квадратной катушки, чем у круглой. При учете толщины разница между катушками меньше, чем без учета толщины. В дальнейших исследованиях полученные теоретические расчеты распределения магнитной индукции катушки Гельмгольца будут применены для анализа экспериментальных данных. Также на основе данных расчетов будет разработан лабораторный прототип для магнитной сепарации на основе катушки Гельмгольца.

**Ключевые слова:** катушка Гельмгольца, закон Био-Савара-Лапласа, однородность магнитного поля, генератор магнитного поля, вычислительная модель

**Introduction.** Currently, Helmholtz coils have found wide application in various fields of technology due to the design of systems with a controlled uniform magnetic field on their basis and their universal and simple design. "Helmholtz coil" refers to two uniaxial coils located in parallel planes at a distance equal to their radius. The currents in each coil are directed so that the magnetic fields in the center of the two coils add up and reinforce each other (Schill & Hoff, 2001). If using round coils, the distance between them should be equal to their average radius. When using square coils, this distance is 0.5445 – a multiple of the length of one side of the coil (Schill & Hoff, 2001). This distance ensures optimal homogeneity of the magnetic field over the entire area.

Helmholtz coils are used in many technical applications. For example, in (Haghnegahdar et al., 2014), the effective use of pulsed electromagnetic fields created by Helmholtz coils was demonstrated to accelerate the healing process of periodontitis. Helmholtz coils are also of great interest for experiments in space biology (Fontanet, Marcos, & Ribó, 2019; Martino et al., 2010) due to their ability to neutralize the Earth's magnetic field and conduct various abiotic and biological experiments. A system with a controlled magnetic field based on a Helmholtz coil has also found wide application in medicine (Brendan et al., 2015).

Large-area coils are mainly used to nullify the Earth's magnetic field. Thus, many studies aim to optimize Helmholtz coils' design to create more efficient and cost-effective solutions with a

larger functional area (Sadiq & Oluyombo, 2019). Such Helmholtz coils are actively used to calibrate magnetic fluxgate magnetometers, where the uniformity of magnetic fields is critically important. These magnetometers are used in geomagnetic observatories to study phenomena associated with geomagnetic storms and the solar-terrestrial system. However, it should be noted that commercial large-area Helmholtz coils are very expensive, and alternative Helmholtz coil systems are needed to create more efficient coils with a smaller area suitable for testing energy systems (Saqib, Francis, & Francis, 2020; Wang, She, & Zhang, 2002).

One of the new applications of the Helmholtz coil is the control of magnetic microrobots (Ramos-Sebastian & Kim, 2021). To implement the control, systems of three pairs of coils, or so-called 3D coils, were created. The main advantage of these systems is the ability to create a uniform magnetic field and a field gradient. These three-dimensional structures for controlled magnetic field generation in any direction are also used for a detailed characterization of the response of Hall probes (Fontanet et al., 2019). Control of ferromagnetic particles using a controlled magnetic field can be applied in oncological research (Kang et al., 2024) and the separation of magnetic particles (Valeev et al., 2019).

For controlled and repeatable impact on experimental samples, creating a given spatial distribution of a uniform magnetic field is necessary. For these purposes, several studies (Hereceg, Juhas, & Milutinov, 2009; Azpurua, 2012; Study and analysis..., n.d.) on the influence of the Helmholtz coil geometry on the level of intensity and uniformity of the magnetic field were conducted, mainly comparing round and square pairs of coils. This relationship between the magnetic field parameters and the physical parameters of the Helmholtz coil will allow the creation of universal laboratory setups. Thus, to calibrate magnetic field sensors used in small satellites such as CubeSats in (Hurtado-Velasco & Gonzalez-Llorente, 2016; Batista et al., 2018; Restrepo et al., 2017), a set of studies was carried out, including both modeling and experimental study of a square Helmholtz coil to determine the magnitude and direction of the magnetic field at any point around the coil. In addition to square and round coil geometries, there are also triangular Helmholtz coils; in the article (Restrepo et al., 2017), comparative calculations of three different geometries with the same coil perimeter were carried out. The results demonstrated high homogeneity of the Helmholtz circular coil. However, these studies did not take into account the thickness of the copper wires and insulation, as well as the arrangement of the turns. In (Crosser et al., 2010), the influence of gaps between adjacent layers of windings caused by the insulation of copper wires was demonstrated in the study of the magnetic field in the geometric center between the coils. Indeed, the influence of the winding location on the intensity of the uniform field is a very important problem. In (Beiranvand, 2017), a study was conducted on the impact of deformation of the cross-sectional shape of small coils on the generated magnetic field, and its homogeneity and optimized system dimensions with increased field homogeneity were proposed.

Thus, at present, many works are devoted to studying the physical parameters of Helmholtz coils and comparing different coil geometries. Still, the lack of comprehensive studies motivates further study of systems based on Helmholtz coils.

This paper presents a comparative study of magnetic field homogeneity and intensity for the most popular Helmholtz coil geometries, supported by the thickness and arrangement of the turns. In addition, this paper presents simplified expressions for the calculations of round and square coils. In this study, for the first time, the influence of both the conductor thickness and the spatial arrangement of the turns was taken into account in the comparative analysis of Helmholtz coil geometries on the homogeneity and magnitude of the generated magnetic field.

*Methods.* The study of the homogeneity and intensity of the magnetic field created by Helmholtz coils with a given current distribution was carried out according to the Biot-Savart-Laplace law:

$$B = \frac{\mu_0}{4\pi} \int \frac{[jI dV, \vec{r}]}{|\vec{r}|^3}, \quad (1)$$

where  $B$  is the magnetic induction vector;  $r$  – a vector drawn from a given infinitesimal volume element  $dV$  to the desired point at which the magnitude of the magnetic field is determined;  $jI$  is the current density  $I$  (the index  $I$  was introduced to avoid repetition with one of the vectors of the basis of the Cartesian coordinate system, namely with the vector  $j$ ).

*Construction of equations for determining magnetic induction for square and round Helmholtz coils without taking into account the thickness and arrangement of turns*

To perform the calculations, the following constants were introduced: the radius of round coils is  $R$ , the length of square coils is  $L$ , the magnetic constant is  $\mu_0$ , and Cartesian coordinate systems are  $x, y, z$ . The case of coils with the same number of turns and the same current value is considered.

The equation of one circular ring of the Helmholtz coil, determined on the basis of the diagram shown in Figure 1:

$$B = \frac{\mu_0}{4\pi} IR \int_0^{2\pi} \frac{(iz \cos a + jz \sin a + k(R - y \sin a - x \cos a)) da}{((x - R \cos a)^2 + (y - R \sin a)^2 + z^2)^{1.5}}. \quad (2)$$

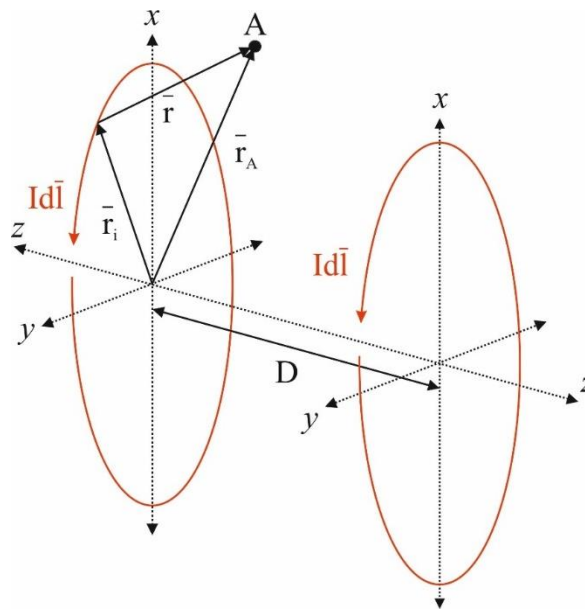


**Figure 1.** Schematic diagram of a circular Helmholtz coil

*Note – compiled by the author*

The equation of one square ring of the Helmholtz coil, defined according to Figure 2:

$$\begin{aligned} B &= B_x i + B_y j + B_z k \\ B_x &= z(F_2 - F_4) \\ B_y &= z(F_3 - F_1) \\ B_z &= \left(y + \frac{L}{2}\right) F_1 - \left(x - \frac{L}{2}\right) F_2 - \left(y - \frac{L}{2}\right) F_3 + \left(x + \frac{L}{2}\right) F_4, \end{aligned} \quad (3)$$

where

$$F_{1,3} = \frac{1}{z^2 + (y \pm \frac{L}{2})^2} \left( \frac{x + \frac{L}{2}}{\sqrt{z^2 + (y \pm \frac{L}{2})^2 + (x + \frac{L}{2})^2}} - \frac{x - \frac{L}{2}}{\sqrt{z^2 + (y \pm \frac{L}{2})^2 + (x - \frac{L}{2})^2}} \right),$$

$$F_{2,4} = \frac{1}{z^2 + (x \mp \frac{L}{2})^2} \left( \frac{y + \frac{L}{2}}{\sqrt{z^2 + (x \mp \frac{L}{2})^2 + (y + \frac{L}{2})^2}} - \frac{y - \frac{L}{2}}{\sqrt{z^2 + (x \mp \frac{L}{2})^2 + (y - \frac{L}{2})^2}} \right).$$

**Figure 2.** Schematic diagram of a square Helmholtz coil

*Note – compiled by the author*

The equation of the magnetic induction vector for two rings (Helmholtz coil) is calculated using the superposition principle:

$$B(z) = B^{(1)}(z) + B^{(1)}(z - D), \quad (4)$$

where  $B^{(1)}$  is determined by formula (2) or formula (3). The magnetic induction vector can be approximately found for coils with  $N$  turns by multiplying the value from formula (4) by  $N$ .

Calculations of the magnetic induction vector of Helmholtz coils are carried out at the same current value, number of turns, perimeter ( $4L = 2\pi R$ ), and the optimal distance between them.

The optimal distance between round coils is equal to their radius; for square coils, it is approximately equal to  $0.5445L$ .

All calculations of magnetic induction and field homogeneity for different Helmholtz coil geometries were performed using the Python programming language with numerical integration, which made it possible to accurately take into account the influence of the conductor thickness and the arrangement of the turns on the magnetic field distribution.

*Results and Analysis. Comparison of magnetic fields taking into account the thickness and arrangement of the turns*

The formulas below, taking into account the thickness of the coil, are also derived from the Biot-Savart law. The thickness of the wire is designated as  $2\delta$ , and the thickness of the insulation is designated as  $2s$  (the thickness of the wire and insulation is determined according to Figure 3).

The equation of one circular ring taking into account the thickness, determined according to Figure 3:

$$B = C \int_{\varphi, \rho, z' = \dots}^{\varphi, \rho, z' = \dots} \frac{(i(z-z')\cos\varphi + j(z-z')\sin\varphi + k(\rho - y\sin\varphi - x\cos\varphi))\rho d\varphi d\rho dz'}{((x-\rho\cos\varphi)^2 + (y-\rho\sin\varphi)^2 + (z-z')^2)^{1.5}}, \quad (5)$$

where

$$C \int_{\varphi, \rho, z'=\dots}^{\varphi, \rho, z'=\dots} = \frac{\mu_0}{4\pi} \frac{I}{\pi \delta^2} \int_{\varphi=0}^{2\pi} \int_{\rho=R-\delta}^{R+\delta} \int_{z'=-\sqrt{\delta^2-(\rho-R)^2}}^{\sqrt{\delta^2-(\rho-R)^2}}$$

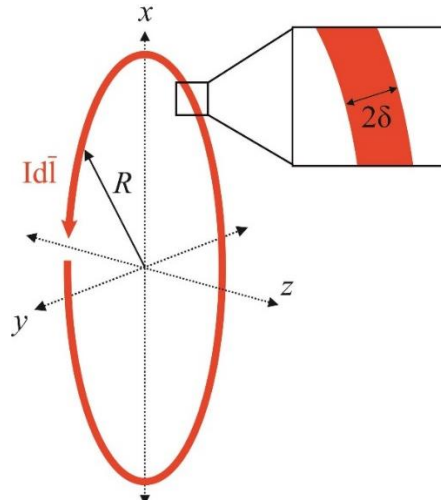


**Figure 3.** Schematic of one ring of a circular Helmholtz coil taking into account the thickness  
Note – compiled by the author

The equation of one square ring taking into account the thickness according to Figure 4:

$$B = \sum_{i=1}^4 (B_i + B'_i), \quad (6)$$

where

$$B_{1,3} = C \int_{\varphi, \rho, z'=\dots}^{\varphi, \rho, z'=\dots} \frac{\left( \mp j(z - \rho \sin \varphi) \pm k \left( y \pm \left( \frac{L}{2} + \delta \right) - \rho \cos \varphi \right) \right) \rho d\varphi d\rho dz'}{\left( (z - \rho \sin \varphi)^2 + \left( y \pm \left( \frac{L}{2} + \delta \right) - \rho \cos \varphi \right)^2 + \left( x + \frac{L}{2} - z' \right)^2 \right)^{1.5}}$$

$$B_{2,4} = C \int_{\varphi, \rho, z'=\dots}^{\varphi, \rho, z'=\dots} \frac{\left( \pm i(z - \rho \sin \varphi) \mp k \left( x \mp \left( \frac{L}{2} + \delta \right) - \rho \cos \varphi \right) \right) \rho d\varphi d\rho dz'}{\left( (z - \rho \sin \varphi)^2 + \left( x \mp \left( \frac{L}{2} + \delta \right) - \rho \cos \varphi \right)^2 + \left( y + \frac{L}{2} - z' \right)^2 \right)^{1.5}}$$

$$C \int_{\varphi, \rho, z'=\dots}^{\varphi, \rho, z'=\dots} = \frac{\mu_0}{4\pi} \frac{I}{\pi \delta^2} \int_{\varphi=0}^{2\pi} \int_{\rho=0}^{\delta} \int_{z'=0}^L$$

$$B'_{1,3} = \int_{\varphi_1=-\frac{\pi}{2}; \varphi_3=\frac{\pi}{2}}^{0; \pi} \left( C \int_{\rho, z'=\dots}^{\rho, z'=\dots} \right)'$$

$$\frac{\left( i(z - z') \cos \varphi + j(z - z') \sin \varphi + k \left( \rho - \left( y \pm \left( \frac{L}{2} + \delta \right) \right) \sin \varphi - \left( x \mp \left( \frac{L}{2} + \delta \right) \right) \cos \varphi \right) \rho d\varphi d\rho dz'}{\left( \left( x \mp \left( \frac{L}{2} + \delta \right) - \rho \cos \varphi \right)^2 + \left( y \pm \left( \frac{L}{2} + \delta \right) - \rho \sin \varphi \right)^2 + (z - z')^2 \right)^{1.5}}$$

$$B'_{2,4} = \int_{\varphi_2=0; \varphi_4=\pi}^{\frac{\pi}{2}; \pi+\frac{\pi}{2}} \left( C \int_{\rho, z'=\dots}^{\rho, z'=\dots} \right)'$$

$$\left( i(z - z') \cos \varphi + j(z - z') \sin \varphi + k \left( \rho - \left( y \mp \left( \frac{L}{2} + \delta \right) \right) \sin \varphi - \left( x \mp \left( \frac{L}{2} + \delta \right) \right) \cos \varphi \right) \right) \rho d\varphi d\rho dz'$$

$$\frac{\left( \left( x \mp \left( \frac{L}{2} + \delta \right) - \rho \cos \varphi \right)^2 + \left( y \mp \left( \frac{L}{2} + \delta \right) - \rho \sin \varphi \right)^2 + (z - z')^2 \right)^{1.5}}{\left( c \int_{\rho, z' = \dots}^{\rho, z' = \dots} \right)' = \frac{\mu_0}{4\pi} \frac{I}{\pi \delta^2} \int_{\rho=0}^{2\delta} \int_{z'=-\sqrt{\delta^2 - (\rho - \delta)^2}}^{\sqrt{\delta^2 - (\rho - \delta)^2}}$$

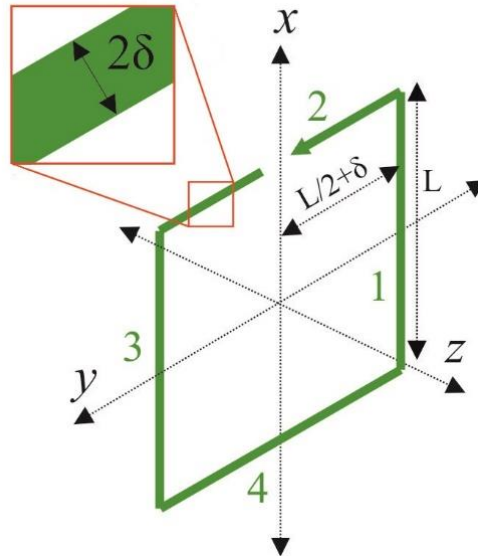


**Figure 4.** Schematic of one ring of a square Helmholtz coil taking into account the thickness  
*Note – compiled by the author*

The resulting magnetic field is calculated using formula (7), where the values of  $N_a$  and  $N_b$  are defined in Figure 5.

If  $N_a$  is an even number, then

$$B = \sum_{k=1}^{N_b} \left( \sum_{j=1}^{N_b} \left( \sum_{i=1}^{\frac{N_a}{2}} [B(z + (\delta + s)(-1)^k + 2(\delta + s)(i - 1)(-1)^k, G)] \right) \right),$$

$$G = R + 2(\delta + s)(j - 1),$$

$$G = 2 \left( \frac{L}{2} + 2(\delta + s)(j - 1) \right).$$

If  $N_a$  is an odd number, then

$$B = B(z, R) + \sum_{k=1}^{N_b} \left( \sum_{j=1}^{N_b} \left( \sum_{i=1}^{\frac{N_a-1}{2}} [B(z + 2i(\delta + s)(-1)^k, G)] \right) \right),$$

$$B = B(z, R) + \sum_{k=1}^{N_b} \left( \sum_{j=1}^{N_b} \left( \sum_{i=1}^{\frac{N_a-1}{2}} (B(z + 2i(\delta + s)(-1)^k, R + 2(\delta + s)(j - 1))) \right) \right), \quad (7)$$

For square and round coils, the values are calculated on the  $z$ -axis at  $x=y=0$ , with the same perimeter  $4L + 2\pi\delta = 2\pi R$ , the same current ( $I=3$  A), the number of turns  $N_a = N_b = 20$  and at the optimal distance. Insulation thickness is  $s = 0.1$  mm, and the wire thickness is  $\delta = 1.4$  mm.

The optimal distance for a round coil is defined as:

$$D = R + N_b(\delta + s). \quad (8)$$

For a square coil, the optimal distance is calculated using the equation:

$$D = 0.5445(L + 2N_b(\delta + s)). \quad (9)$$

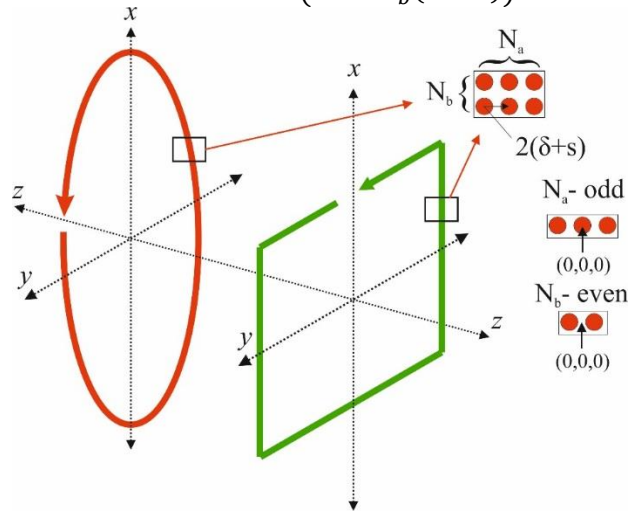


**Figure 5.** Taking into account the arrangement of turns  $\delta$  and the thickness of the insulation  $s$ .

*Note – compiled by the author*

The calculations were obtained by integrating using the Newton-Cotes formula (a second-degree polynomial was used). The relative errors are determined using the Runge method as  $\frac{|I_{2h} - I_h|}{I_{2h}}$  (where  $I_h$  is the approximately calculated integral with the number of steps  $h$ ), are less than 0.5% for all calculated values.

For a more visual comparison, we will place the center of the coordinate system in the middle between the rings, i.e., the formulas above use the value  $B(z) = B\left(z + \frac{D}{2}\right)$ .

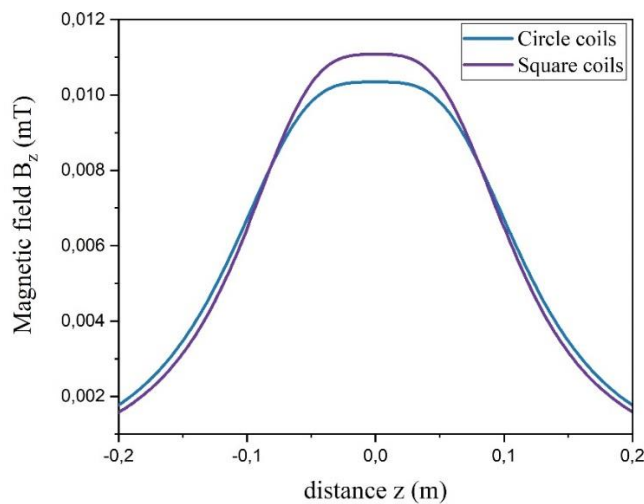


**Figure 6.** Distribution of the magnetic field of a pair of round and square Helmholtz coils on the  $z$ -axis

*Note – compiled by the author*

Figure 6 shows a comparison of the magnetic field intensity of a round and square coil. A



comparison of the magnetic field homogeneity is shown in Figure 7.

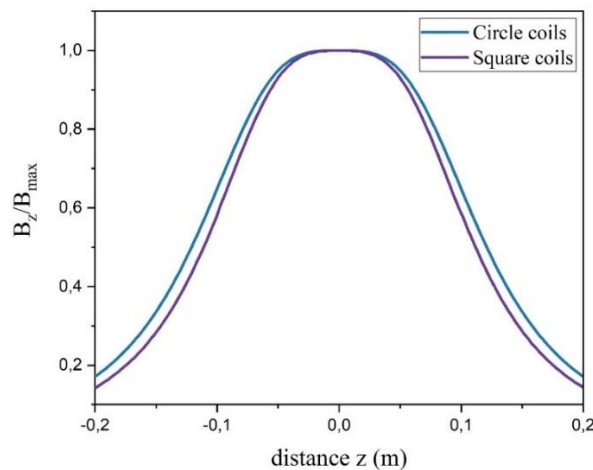


**Figure 7.** Normalized distribution of the magnetic field of a pair of round and square Helmholtz coils  
Note – compiled by the author

From the graphs shown in Figures 6 and 7, it is evident that the homogeneity zone is better for the round coil. The absolute value is higher for the square coil ( $\frac{B_{z,KB}(z=0)}{B_{z,KP}(z=0)} \approx 1.07$ , i.e., a 7% stronger field, without taking into account the thickness of the coil  $\frac{B_{z,KB}(z=0)}{B_{z,KP}(z=0)} \approx 1.1532$ ). For a round coil, the relative distance at which the field is 99% of the maximum is  $\frac{z}{R+N_b(\delta+s)} \approx 0.29$  (0.3137 excluding the coil thickness), for a square coil it is  $\frac{z}{R+N_b(\delta+s)} \approx 0.26$  (0.2692 excluding the coil thickness), the difference between the relative distances taking into account the thickness is  $\frac{0.29}{0.26} \approx 1.1154$  or 12% (17% excluding the coil thickness).

**Conclusions.** This research paper describes the basic theoretical measurements of the magnetic induction generated by a round and square Helmholtz coil, taking into account the thickness and arrangement of the turns and a comparison of their magnetic induction. Calculations show that the value of the homogeneity zone of the round coil is larger than that of the square coil, but the magnetic induction in this zone is larger for the square coil than for the round coil. When taking into account the thickness, the difference between the coils is smaller than without taking into account the thickness.

In future studies, the obtained theoretical calculations of the distribution of magnetic induction of the Helmholtz coil will be experimentally compared. Based on the theoretical calculations, a laboratory prototype based on a Helmholtz coil is being developed for the magnetic separation of industrial fly ash.

**Acknowledgments.** This research has been funded by the Ministry of Science and Higher Education of the Republic of Kazakhstan (Grant No. BR21882301)

#### References

- Schill, R. A., Jr., Hoff, K. (2001). Characterizing and calibrating a large Helmholtz coil at low AC magnetic field levels with peak magnitudes below the earth's magnetic field. *Review of Scientific Instruments*, 72(6), 2769–2776, <https://doi.org/10.1063/1.1368853>.
- Haghnegahdar, A., Khosrovpanah, H., Andisheh-Tadbir, A., Mortazavi, G. (2014). Design and fabrication of Helmholtz coils to study the effects of pulsed electromagnetic fields on the healing process in periodontitis: Preliminary animal results. *Journal of Biomedical Physics & Engineering*, 4(3), 83–90.

- Fontanet, A., Marcos, J., Ribó, L. (2019). Design and construction of 3D Helmholtz coil system to calibrate 3D Hall probes. *Journal of Physics: Conference Series*, 1350, 012167, <https://doi.org/10.1088/1742-6596/1350/1/012167>.
- Martino, C. F., Portelli, L., McCabe, K., Hernandez, M., Barnes, F. (2010). Reduction of the earth's magnetic field inhibits growth rates of model cancer cell lines. *Bioelectromagnetics*, 31(7), 649–655, <https://doi.org/10.1002/bem.20606>.
- Brendan, D., Watson, J. C., Bartlett, P., Renzoni, F. (2015). Toward an automated setup for magnetic induction tomography. *IEEE Transactions on Magnetics*, 51(1), 1–4, <https://doi.org/10.1109/TMAG.2014.2355420>.
- Sadiq, U. A., Oluyombo, O. W. (2019). Optimization design and characterization of Helmholtz coils. *Journal of Information Engineering and Applications*, 9(4), <https://doi.org/10.7176/JIEA/9-4-05>.
- Saqib, M., Francis, S. N., Francis, J. N. (2020). Design and development of Helmholtz coils for magnetic field. In *International Youth Conference on Radio Electronics, Electrical and Power Engineering (REEPE)*, 1–5, <https://doi.org/10.1109/REEPE49198.2020.9059109>.
- Wang, J., She, S., Zhang, S. (2002). An improved Helmholtz coil and analysis of its magnetic field homogeneity. *Review of Scientific Instruments*, 73(6), 2175–2179, <https://doi.org/10.1063/1.1471352>.
- Ramos-Sebastian, A., Kim, S. H. (2021). Magnetic force-propelled 3D locomotion control for magnetic microrobots via simple modified three-axis Helmholtz coil system. *IEEE Access*, 9, 128755–128764, <https://doi.org/10.1109/ACCESS.2021.3113765>.
- Fontanet, A., Marcos, J., Ribó, L., Massana, V., Campmany, J. (2019). Design and construction of 3D Helmholtz coil system to calibrate 3D Hall probes. *Journal of Physics: Conference Series*, 1350, 012167, <https://doi.org/10.1088/1742-6596/1350/1/012167>.
- Kang, K., Lee, S. Y., Kim, C. S., Park, C. H. (2024). Hybrid magnetic field system with Helmholtz coils and magnets for real-time circulating tumor cell separation. *Sensors and Actuators A: Physical*, 370, 115229, <https://doi.org/10.1016/j.sna.2024.115229>.
- Valeev, D., Kunilova, I., Alpatov, A., Varnavskaya, A., Ju, D. (2019). Magnetite and carbon extraction from coal fly ash using magnetic separation and flotation methods. *Minerals*, 9(5), 320, <https://doi.org/10.3390/min9050320>.
- Herceg, D., Juhas, A., Milutinov, M. (2009). A design of a four square coil system for a biomagnetic experiment. *Facta Universitatis Series: Electronics and Energetics*, 22(3), 285–292.
- Azpuru, M. A. (2012). A semi-analytical method for the design of coil systems for homogeneous magnetostatic field generation. *Progress in Electromagnetics Research B*, 37, 171–189.
- Study and analysis of magnetic field homogeneity of square and circular Helmholtz coil pairs: A Taylor series approximation. (n.d.).
- Hurtado-Velasco, R., Gonzalez-Llorente, J. (2016). Simulation of the magnetic field generated by square shape Helmholtz coils. *Applied Mathematical Modelling*, 40(23–24), 9835–9847, <https://doi.org/10.1016/j.apm.2016.06.027>.
- Batista, D. S., Granziera, F., Tosin, M. C., de Melo, L. F. (2018). Three-axial Helmholtz coil design and validation for aerospace applications. *IEEE Transactions on Aerospace and Electronic Systems*, 54(1), 392–403, <https://doi.org/10.1109/TAES.2017.2760560>.
- Restrepo, A. F., Franco, E., Cadavid, H., Pinedo, C. R. (2017). A comparative study of the magnetic field homogeneity for circular, square and equilateral triangular Helmholtz coils. In *2017 International Conference on Electrical, Electronics, Communication, Computer, and Optimization Techniques (ICEECOT)* (pp. 13–20), <https://doi.org/10.1109/ICEECOT.2017.8284514>.
- Crosser, M. S., Scott, S., Clark, A., Wilt, P. M. (2010). On the magnetic field near the center of Helmholtz coils. *Review of Scientific Instruments*, 81(8), 084701, <https://doi.org/10.1063/1.3474227>.
- Beiranvand, R. (2017). Effects of the winding cross-section shape on the magnetic field uniformity of the high field circular Helmholtz coil. *IEEE Transactions on Industrial Electronics*, 64(9), 7120–7131, <https://doi.org/10.1109/TIE.2017.2686302>.

#### Information about authors

**Zhakypov Alibek** – Master of Engineering and Technology, Al-Farabi Kazakh National University, Almaty, Kazakhstan, E-mail: szhakupovalibek@gmail.com, ORCID: 0009-0001-9904-318X, +7 705 141 65 69

**Zhumanov Temirkhan** – Undergraduate student, 4th year, Al-Farabi Kazakh National University, Almaty, Kazakhstan, E-mail: szhakupovalibek@gmail.com, +7 701 773 77 24

**Akhanova Nazym** – PhD, Kazakh-British Technical University, E-mail: nazym@physics.kz, ORCID: 0000-0003-2767-8711, +7 707 783 96 55

**Sultangazina Marzhan** – Master of Engineering and Technology, Al-Farabi Kazakh National University, Almaty, Kazakhstan, E-mail: marjan\_0309@mail.ru, ORCID: 0000-0002-8162-096X, +7 777 807 88 11

**Gabdullin Maratbek** – Candidate of Physical and Mathematical Sciences, PhD, Professor, Kazakh-British Technical University, E-mail: m.gabdullin@kbtu.kz, ORCID: 0000-0003-2767-8711, +7 777 807 88 11